Supporting Information

Biotin-decorated hollow gold nanoshell for dual-modal imaging-guided NIR-II photothermal and radiosensitizing therapy toward breast cancer

Yongjian Chen[a,1], Wei Meng[a,1], Ming Chen[b,1], Lianying Zhang[c], Mingwa Chen[a], Xiaotong Chen[a], Jian Peng[a], Naihan Huang[a], Wenhua Zhang[d,*], Jinxiang Chen[a,*]

[a] Guangdong Provincial Key Laboratory of New Drug Screening, Guangzhou Key Laboratory of Drug Research for Emerging Virus Prevention and Treatment, NMPA Key Laboratory for Research and Evaluation of Drug Metabolism, School of Pharmaceutical Sciences, Southern Medical University, Guangzhou, Guangdong 510515, China.

[b] The People's Hospital of Gaozhou, Maoming 525200, China

[c] School of Pharmacy Sciences, Southwest Medical University, Luzhou 646000, China

[d] College of Chemistry, Chemical Engineering and Materials Science, Soochow University, Suzhou 215123, People's Republic of China

[1] These authors contributed equally to this work.

* Corresponding authors.

E-mail: whzhang@suda.edu.cn (W. H. Zhang); jxchen@smu.edu.cn (J. X. Chen)

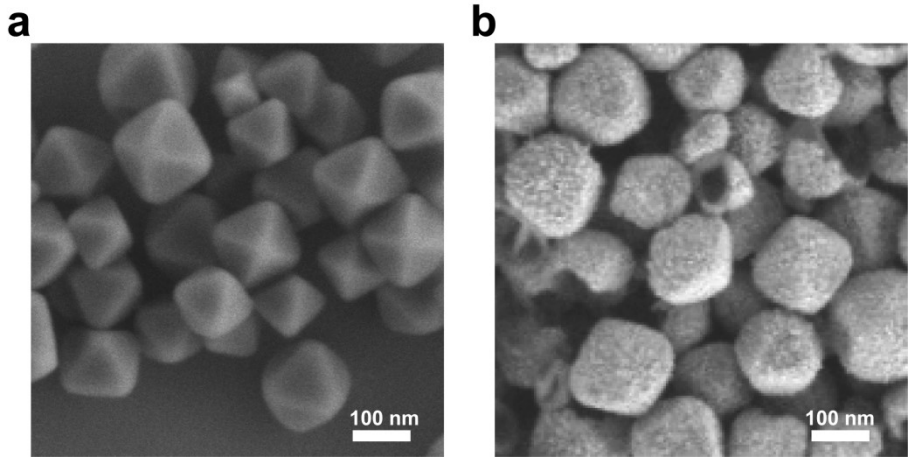

Fig. S1. (a) The SEM images of (a) UiO-66-NH_2 and (b) HAuNS@PEG-bio nanoparticles.

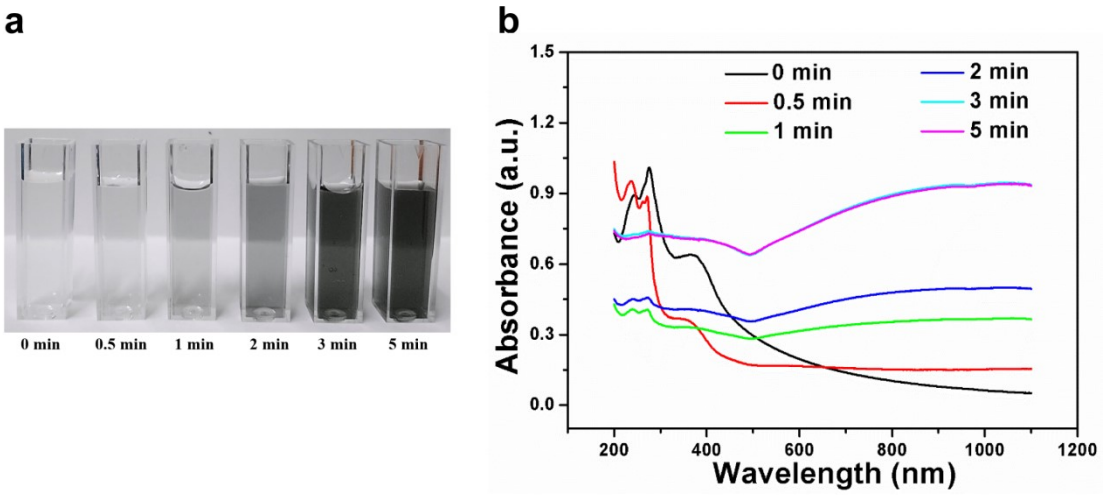

Fig. S2. (a) The corresponding color change and its (b) UV-Vis-NIR spectra of UiO-66-NH_2@AuNS solution at different reaction time.

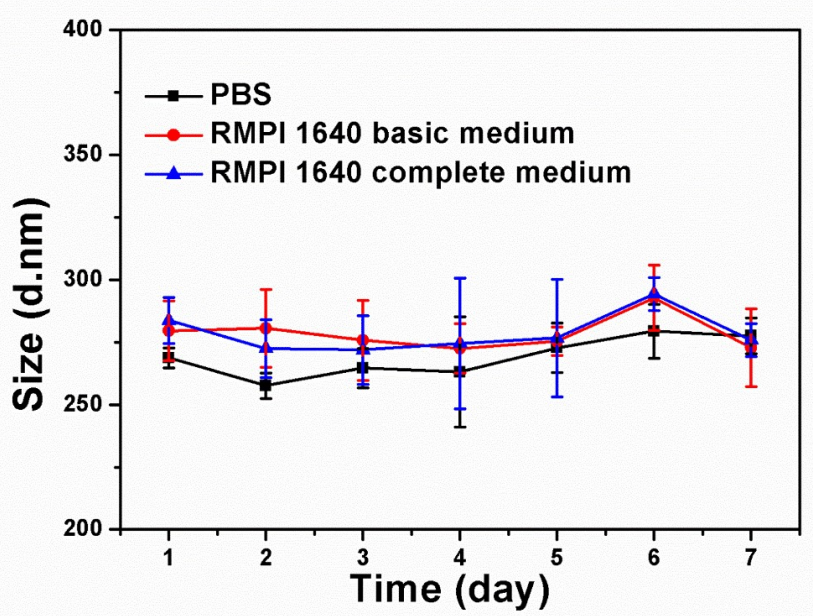

Fig. S3. Size changes of HAuNS@PEG-bio in different media (PBS, RMPI 1640 basic medium, and RMPI 1640 complete medium at designed pointed during 7 days measured by dynamic light scattering.

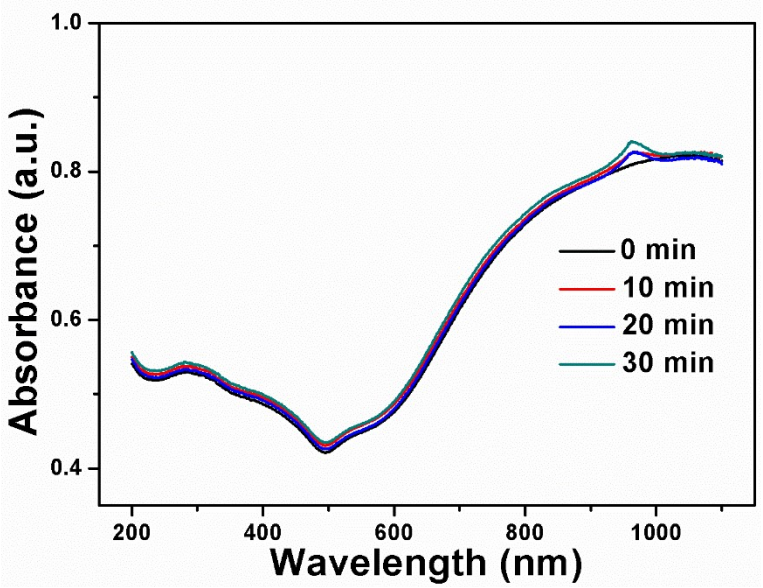

Fig. S4. The UV-Vis-NIR spectra of HAuNS@PEG-bio at the concentration of 160 μg mL^{-1} irradiated by 1064 nm laser with a power density of 1 W cm^{-2} during 0, 10, 20, and 30 min.

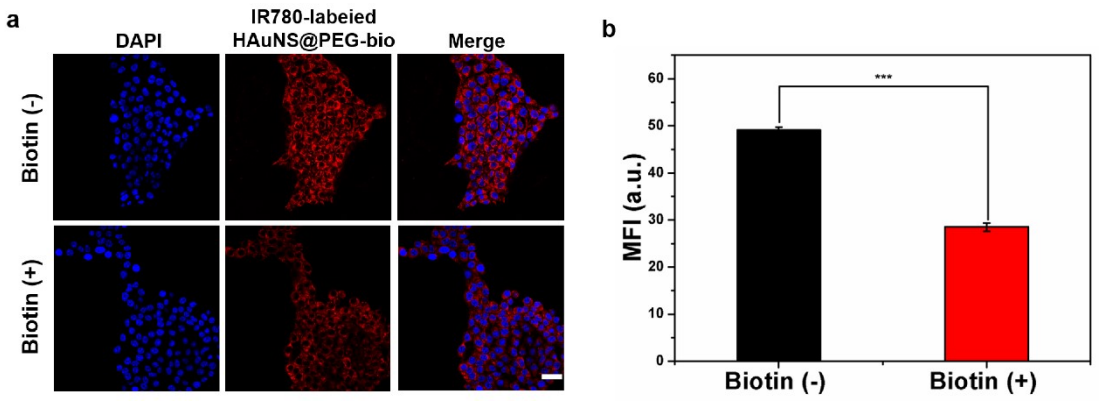

Fig. S5. (a) The cellular uptake CLSM images of IR780-labeled HAuNS@PEG-bio and IR780-labeled HAuNS@PEG-bio + biotin and (b) its mean fluorescence intensity. Scale bar = 40 μm. (***P<0.001)

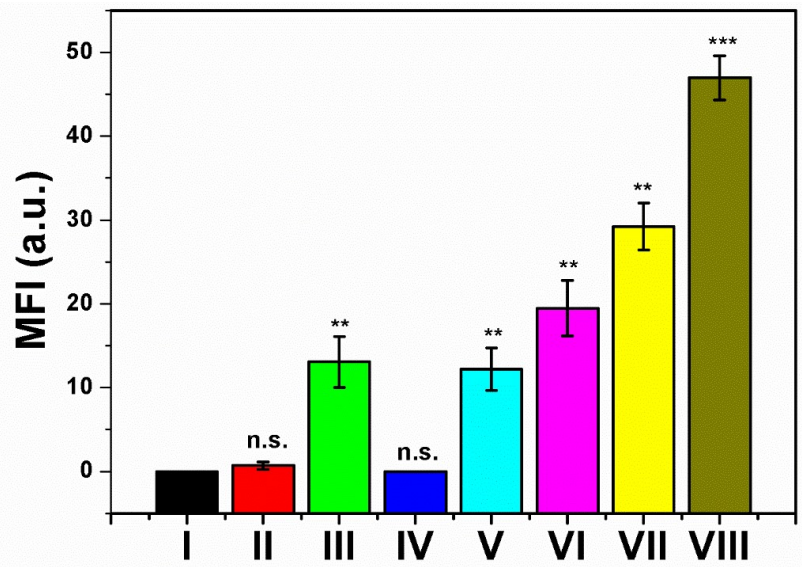

Fig. S6. The mean fluorescence intensity (MFI) of ROS generation in 4T1 cells after different treatments. n.s. P>0.05, *P<0.05, **P<0.01, ***P<0.001 *vs* PBS group. (I: PBS; II: PBS + PTT; III: PBS + RT; IV: HAuNS@PEG-bio; V: HAuNS@PEG-bio + PTT; VI: HAuNS@PEG-bio + RT; VII: HAuNS + PTT + RT; VIII: HAuNS@PEG-bio + PTT + RT)

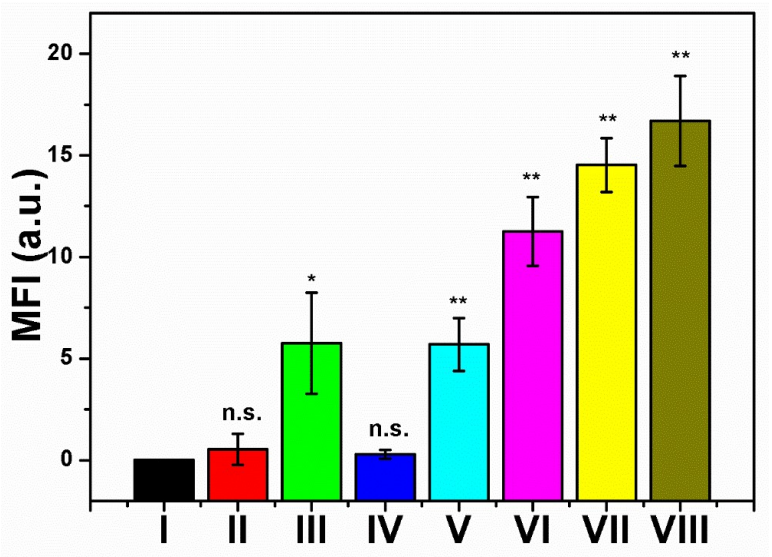

Fig. S7. The mean fluorescence intensity of γ-H2AX in 4T1 cells after different treatments. n.s. P>0.05, *P<0.05, **P<0.01, ***P<0.001 *vs* PBS group. (I: PBS; II: PBS + PTT; III: PBS + RT; IV: HAuNS@PEG-bio; V: HAuNS@PEG-bio + PTT; VI: HAuNS@PEG-bio + RT; VII: HAuNS + PTT + RT; VIII: HAuNS@PEG-bio + PTT + RT)

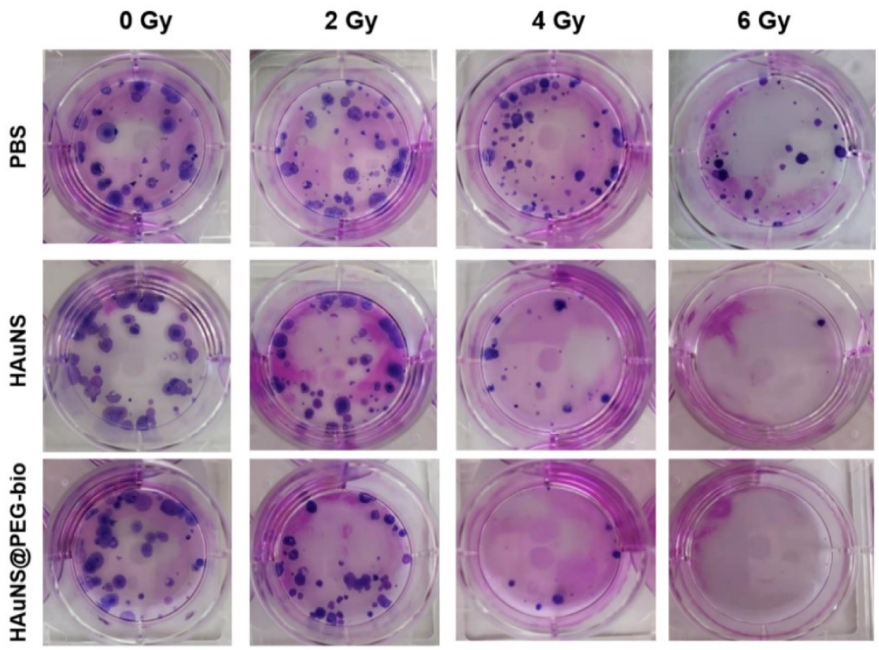

Fig. S8. Photographs of colony formation assay of 4T1 cells treated with PBS, HAuNS, and HAuNS@PEG-bio nanoparticles under various radiation dose (0, 2, 4, and 6 Gy).

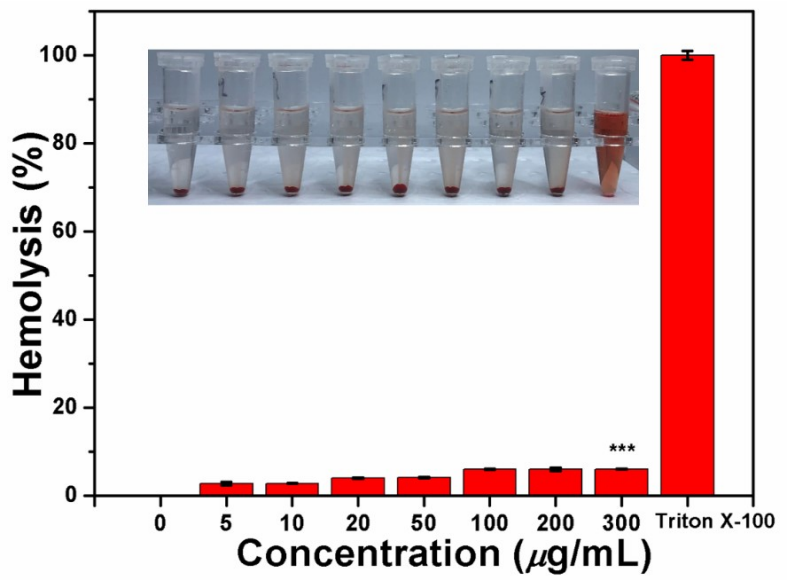

Fig. S9. The hemolytic of HAuNS@PEG-bio at different concentration. Data was presented as the mean ± SD (n = 3). (***p<0.001)

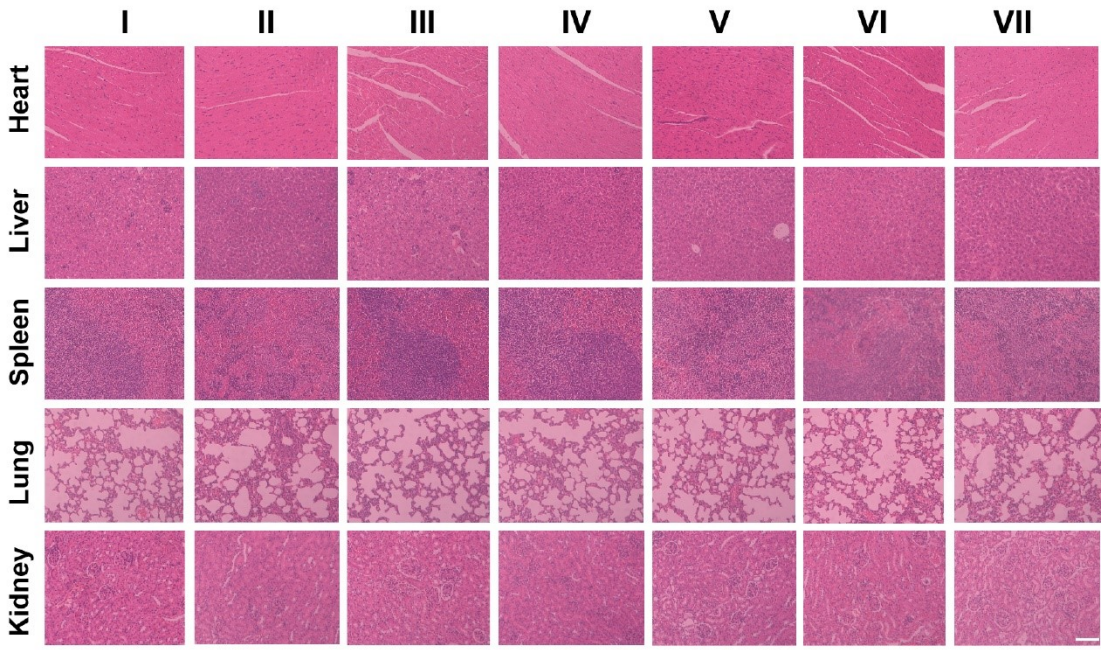

Fig. S10. H&E staining of main organs (heart, liver, spleen, lung and kidney) tissue slices after different treatments. Scale bars = 200 μm. (I: PBS; II: PBS + PTT + RT; III: HAuNS@PEG-bio; IV: HAuNS@PEG-bio + PTT; V: HAuNS@PEG-bio + RT; VI: HAuNS + PTT + RT; VII: HAuNS@PEG-bio + PTT + RT)

Table S1. Photothermal conversion efficiencies of reported Au-based nanoagents.

Materials	**Laser (nm)**	**Power (W/cm^2)**	**η（%）**	**References**
UCNPs@mSiO$_2$-Au-Cys nanomotors	808	1.5	28	[1]
BAuNSP (branched nanoporous gold nanoshells)	808	1	75.5	[2]
Hollow gold nanoshell-coupled silica microrods	808	2	39.6	[3]
Iron oxide@Au/Ag nanoparticles	1064	3.0	28.3	[4]
PMC@AuNP	1064	1	49.3	[5]
Au nanorods	1064	2	22.1	[6]
Au-Cu$_9$S$_5$ nanoparticles	1064	0.7	37	[7]
Porous Au@Pt core-shell nanostructures	1064	1	41.3	[8]
AuNFs (gold nanoframeworks)	1064	1	23.9	[9]
HAuNS@PEG-bio	1064	1	63	this work

References

[1] H. Liu, J. Zhang, Y. Jia, X. Liu, X. Chen, W. Zhao, C. Mao, *Chem. Eng. J.* **2022**, 442, 135994.

[2] J. Song, X. Yang, Z. Yang, L. Lin, Y. Liu, Z. Zhou, Z. Shen, G. Yu, Y. Dai, O. Jacobson, J. Munasinghe, B. Yung, G.-J. Teng, X. Chen, *ACS Nano* **2017**, 11, 6102.

[3] S. Han, Y.-J. Park, E.-J. Park, Y. Kim, *ACS Appl. Mater. Interfaces* **2019**, 11, 8831.

[4] B. Guo, Z. Sheng, D. Hu, C. Liu, H. Zheng, B. Liu, *Advanced Materials* **2018**, 30, 1802591.

[5] C. Du, L. Zhou, J. Qian, M. He, C.-M. Dong, J.-D. Xia, Z.-G. Zhang, R. Zhang, *J. Mater. Chem. B* **2021**, 9, 5484.

[6] J. Zeng, D. Goldfeld, Y. Xia, *Angew. Chem. Int. Edit.* **2013**, 52, 4169.

[7] X. Ding, C. H. Liow, M. Zhang, R. Huang, C. Li, H. Shen, M. Liu, Y. Zou, N. Gao, Z. Zhang, Y. Li, Q. Wang, S. Li, J. Jiang, *J. Am. Chem. Soc.* **2014**, 136, 15684.

[8] J. Sun, J. Wang, W. Hu, Y. Wang, Q. Zhang, X. Hu, T. Chou, B. Zhang, C. Gallaro, M. Halloran, L. Liang, L. Ren, H. Wang, *ACS Nano* **2022**, 16, 10711.

[9] J. Wang, J. Sun, Y. Wang, T. Chou, Q. Zhang, B. Zhang, L. Ren, H. Wang, *Adv. Funct. Mater.* **2020**, 30, 1908825.